

One-Dimensional BeH₂ Polymers: Infrared Spectra and Theoretical Calculations

Xuefeng Wang and Lester Andrews*

Department of Chemistry, University of Virginia, Charlottesville, Virginia 22901

Received November 2, 2004

Laser-ablated beryllium atoms react with H₂ upon co-condensation in excess hydrogen and neon to form BeH₂ and (BeH₂)₂, which are identified through isotopic substitution and DFT calculations. Unreacted Be atoms isolated in solid neon or hydrogen are excited to the ¹P₀ state and react further with H₂ to enhance the BeH₂ and (BeH₂)₂ concentrations and produce (BeH₂)_n polymers. The series of strong infrared-active parallel Be–H–Be bridge-bond stretching modes observed for (BeH₂)_n polymers suggests one-dimensional structures, and this conclusion is supported by DFT calculations. The computed polymerization energy per BeH₂ unit is about 33 kcal/mol.

Introduction

Solid BeH₂ is difficult to prepare, particularly in pure crystalline form, and early attempts have produced amorphous and crystalline forms that evolved hydrogen gas upon heating and were believed to involve flat polymeric chains of bridging hydrides.^{1–4} However, the pure crystal structure has been established by high-resolution X-ray diffraction using synchrotron radiation as body-centered orthorhombic with a network of connected BeH₄ tetrahedra, and there is no known analogue among other compounds containing tetrahedral building blocks.⁵ Structural quantum effects in amorphous solid BeH₂ and BeD₂ have recently been investigated.⁶ Furthermore, DFT structure calculations on crystalline BeH₂⁷ are in agreement with the X-ray analysis.⁵ Although BeH₂ has a high hydrogen storage capacity (18.2 wt %), this solid hydride has been ruled out for commercial hydrogen storage material because of its high toxicity, but it has still attracted considerable interest for nuclear reactor and rocket fuel.^{6–9} Beryllium dihydride is a favorite metal

hydride molecule for theoretical explorations because of the small number of electrons for quantum chemical calculations,^{10–15} which can also give useful information on chemical properties of metal hydride materials, including solid and polymeric beryllium hydrides.^{7,8,10} The linear BeH₂ molecule was first identified in a solid argon matrix at 10 K in 1993 by this group,¹² and 10 years later the gaseous BeH₂ molecule was characterized from infrared emission spectra.¹⁶ We have found no experimental studies on polymeric BeH₂, although a theoretical investigation involving chains to simulate infinite polymers has been reported recently.⁸

Reactions of laser-ablated metal atoms with H₂ in excess molecular hydrogen have provided valuable technology for the study of metal hydrides. Recently, we have prepared dialane, triallane, and indane and explored the chemistry of these binary hydrides in solid hydrogen.^{17–20} After sublima-

* Corresponding author. E-mail: isa@virginia.edu.

- (1) Head, E. L.; Holley, C. E.; Rabideau, S. W. *J. Am. Chem. Soc.* **1957**, *79*, 3687.
- (2) Brendel, G. J.; Marlett, E. M.; Niebylski, L. M. *Inorg. Chem.* **1978**, *17*, 3589 and references therein.
- (3) Greenwood, N. N.; Earnshaw, A. *Chemistry of the Elements*; Pergamon Press: Oxford, U.K., 1984; pp 125–126.
- (4) Cotton, F. A.; Wilkinson, G.; Murillo, C. A.; Bochmann, M. *Advanced Inorganic Chemistry*, 6th ed.; Wiley: New York, 1999; p 115.
- (5) Smith, G. S.; Johnson, Q. C.; Smith, D. K.; Cox, D. E.; Snyder, R. L.; Zhou, R. S.; Zalkin, A. *Solid State Commun.* **1988**, *67*, 491.
- (6) Sampath, S.; Lantzky, K. M.; Benmore, C. J.; Nevefeind, J.; Sievenie, J. E.; Egelstaff, P. A.; Yarger, J. L. *J. Chem. Phys.* **2003**, *119*, 12499.
- (7) Vajeeston, P.; Ravindran, P.; Kjekshus, A.; Fjellvag, H. *Appl. Phys. Lett.* **2004**, *84*, 34.

- (8) Abdurahman, A.; Shukla, A.; Dolg, M. *J. Chem. Phys.* **2000**, *112*, 4801.
- (9) Grochala, W.; Edwards, P. P. *Chem. Rev.* **2004**, *104*, 1283.
- (10) Karpfen, A. *Theor. Chim. Acta* **1978**, *50*, 49.
- (11) (a) Martin, J. M. L.; Lee, T. J. *Chem. Phys. Lett.* **1992**, *200*, 502 and references therein. (b) Martin, J. M. L. *Chem. Phys. Lett.* **1997**, *273*, 98.
- (12) Tague, T. J., Jr.; Andrews, L. *J. Am. Chem. Soc.* **1993**, *115*, 12111 and references therein.
- (13) Szalay, P. G.; Bartlett, R. J. *J. Chem. Phys.* **1995**, *103*, 3600.
- (14) Heinze, J.; Friedrich, O.; Sundermann, A. *Mol. Phys.* **1999**, *96*, 711.
- (15) Jursic, B. S. *J. Mol. Struct. (THEOCHEM)* **1999**, *467*, 7.
- (16) (a) Bernath, P. F.; Shayesteh, A.; Tereszchuk, K.; Colin, R. *Science* **2002**, *297*, 1323. (b) Shayesteh, A.; Tereszchuk, K.; Bernath, P. F.; Colin, R. *J. Chem. Phys.* **2003**, *118*, 3622.
- (17) (a) Andrews, L.; Wang, X. *Science* **2003**, *299*, 2049. (b) Wang, X.; Andrews, L.; Tam, S.; DeRose, M. E.; Fajardo, M. *J. Am. Chem. Soc.* **2003**, *125*, 9218. (c) Andrews, L.; Wang, X. *J. Phys. Chem. A* **2004**, *108*, 4202 (Al+H₂).
- (18) Andrews, L.; Wang, X. *Angew. Chem., Int. Ed.* **2004**, *43*, 1706.

tion of the hydrogen matrix, solid alane and indane films remained on the cold window. Magnesium atom reactions with pure hydrogen gave MgH₂ and Mg₂H₄ in solid hydrogen, and solid MgH₂ was formed upon sublimation of the hydrogen matrix host.²¹

Experimental and Theoretical Methods

Laser-ablated metal atom reactions with hydrogen in excess molecular hydrogen and neon during condensation at 4 K have been described in detail previously.^{20–23} The Nd:YAG laser fundamental (1064 nm, 10-Hz repetition rate with 10-ns pulse width) was focused onto a rotating beryllium target (Johnson Matthey), and the laser energy was varied from 10 to 20 mJ/pulse. FTIR spectra were recorded at 0.5 cm⁻¹ resolution on a Nicolet 750 spectrometer with 0.1 cm⁻¹ accuracy using a mercury cadmium telluride type B detector. Matrix samples were annealed at different temperatures, and selected samples were subjected to photolysis by a medium-pressure mercury arc lamp (Philips, 175 W, globe removed) through optical filters. Complementary DFT calculations were performed using the Gaussian 98 program,²⁴ the B3LYP density functional,²⁵ and the large 6-311++G(3df,3pd) basis set.²⁶

Results and Discussion

Figure 1 illustrates the terminal Be–H and bridge Be–H–Be stretching regions from the infrared spectrum of Be and H₂ reaction products in excess neon and normal hydrogen during condensation at 4 K. Strong absorptions at 2172.2 and 708.5 cm⁻¹ are due to the BeH₂ molecule stretching and bending modes in solid neon based on agreement with argon matrix (2159.1, 697.9 cm⁻¹)¹² and gas-phase (2178.9 cm⁻¹)¹⁶ fundamental band positions and calculated harmonic frequencies [MBPT(2), 2229 and 747 cm⁻¹;¹² B3LYP, 2263 and 724 cm⁻¹] and anharmonic frequencies (CCSD, 2167 and 717 cm⁻¹).¹¹ New absorptions at 1576.9, 1422.9, 922.9, and 584.6 cm⁻¹ were also observed with 4% H₂ in solid neon. These bands increased upon ultraviolet irradiation, and a strong new group of red satellite bands appeared in the Be–

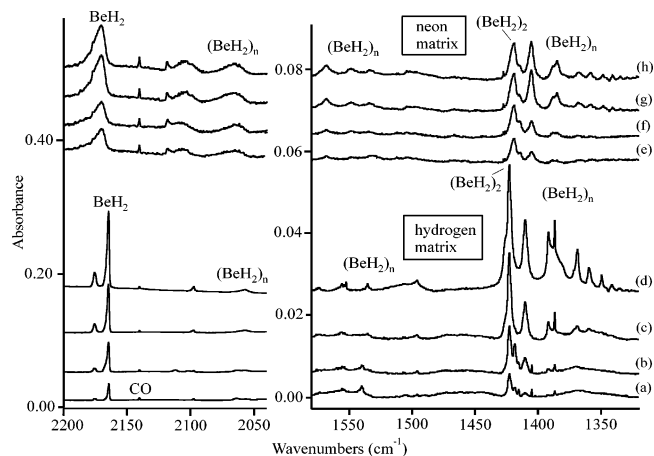


Figure 1. Infrared spectra in the 2200–2040 and 1580–1320 cm⁻¹ regions for laser-ablated Be atoms co-deposited with hydrogen at 4 K: (a) Pure hydrogen, (b) after $\lambda > 350$ nm irradiation, (c) after 240–380 nm irradiation, and (d) after $\lambda > 220$ nm irradiation. (e) Neon with 4% H₂, (f) after $\lambda > 350$ nm irradiation, (g) after $\lambda > 220$ nm irradiation, and (h) after a second $\lambda > 220$ nm irradiation.

Table 1. Infrared Absorptions (cm⁻¹) Observed from Reaction of Beryllium and Dihydrogen in Pure Hydrogen and in Excess Neon

H ₂	D ₂	HD	H ₂ /Ne	D ₂ /Ne	identification
2165.3		2168.4	2172.2		BeH ₂
		2096.4, 1530.6			BeHD
	1678.3	1680.7		1681.7	BeD ₂
2056	1533	2067, 1538	2065	1536	(BeH ₂) _n
2014.2	1510.5	2040.3, 1533.4	2020	1510	HBeBeH
1978.3		1977.7	1983.7		BeH
	1481.4	1481.9		1485.7	BeD
1574.8	1232.0		1576.9	1232.9	(BeH ₂) ₂
1556.0	1219.5		1558.4	1221.2	(BeH ₂) _n
1536.4			1541.1	1186.8	(BeH ₂) _n
1422.7	1098.2		1422.9	1098.5	(BeH ₂) ₂
1410.0	1074.7		1408.1	1073.9	(BeH ₂) _n
1391.7	1058.1		1390.5	1058.0	(BeH ₂) _n
1368.4	1039.7		1368.8	1039.8	(BeH ₂) _n
1359.5	1024		1359.5	1024.3	(BeH ₂) _n
1349.4			1349.2		(BeH ₂) _n
1341.2			1341.3		(BeH ₂) _n
1334.8			1334.8		(BeH ₂) _n
1329.6			1329.4		(BeH ₂) _n
920	685		922.9	685.4	(BeH ₂) ₂
867	654		867	654	(BeH ₂) _n
864			864		(BeH ₂) _n
706.3		703.9	708.5		BeH ₂
		628.8			BeHD
	537.0	539.3		538.2	BeD ₂
			584.6		(BeH ₂) ₂
573			572		(BeH ₂) _n
567			563		(BeH ₂) _n
558			558		(BeH ₂) _n

H–Be stretching region (Table 1). A broad feature at 2065 cm⁻¹ in the Be–H stretching region and weak 867 and 572 cm⁻¹ bands in the Be–H–Be bending region also increased with the latter absorptions. With 4% D₂ in solid neon, all of the bands shifted downward, giving 1.29–1.34 H/D frequency ratios, which are appropriate for light metal hydride vibrations. The absorptions of the HBeD molecule in solid neon are observed at 2101.5, 1534.6, and 629.4 cm⁻¹, with new absorptions in concert at 2067, 1568, 1388, and 1085 cm⁻¹ upon irradiation. In addition, weak bands at 1983.7 cm⁻¹ in H₂/Ne and 1485.7 cm⁻¹ in D₂/Ne can be identified as diatomic BeH and BeD, respectively.⁸

- (19) (a) Wang, X.; Andrews, L. *J. Phys. Chem. A* **2003**, *107*, 11371. (Ga+H₂). (b) Wang, X.; Andrews, L. *J. Phys. Chem. A* **2004**, *108*, 3396 (Ti+H₂). (c) Wang, X.; Andrews, L. *J. Phys. Chem. A* **2004**, *108*, 4440 (In+H₂).
- (20) Andrews, L. *Chem. Soc. Rev.* **2004**, *33*, 123 and references therein.
- (21) Wang, X.; Andrews, L. *J. Phys. Chem. A* **2004**, *108*, 11511.
- (22) Wang, X.; Andrews, L. *J. Phys. Chem. A* **2004**, *108*, 1103.
- (23) Andrews, L.; Citra, A. *Chem. Rev.* **2002**, *102*, 885 and references therein.
- (24) Frisch, M. J.; Trucks, G. W.; Schlegel, H. B.; Scuseria, G. E.; Robb, M. A.; Cheeseman, J. R.; Zakrzewski, V. G.; Montgomery, J. A., Jr.; Stratmann, R. E.; Burant, J. C.; Dapprich, S.; Millam, J. M.; Daniels, A. D.; Kudin, K. N.; Strain, M. C.; Farkas, O.; Tomasi, J.; Barone, V.; Cossi, M.; Cammi, R.; Mennucci, B.; Pomelli, C.; Adamo, C.; Clifford, S.; Ochterski, J.; Petersson, G. A.; Ayala, P. Y.; Cui, Q.; Morokuma, K.; Malick, D. K.; Rabuck, A. D.; Raghavachari, K.; Foresman, J. B.; Cioslowski, J.; Ortiz, J. V.; Stefanov, B. B.; Liu, G.; Liashenko, A.; Piskorz, P.; Komaromi, I.; Gomperts, R.; Martin, R. L.; Fox, D. J.; Keith, T.; Al-Laham, M. A.; Peng, C. Y.; Nanayakkara, A.; Gonzalez, C.; Challacombe, M.; Gill, P. M. W.; Johnson, B.; Chen, W.; Wong, M. W.; Andres, J. L.; Gonzalez, C.; Head-Gordon, M.; Replogle, E. S.; Pople, J. A. *Gaussian 98*, revision A.6; Gaussian, Inc.: Pittsburgh, PA, 1998 and references therein.
- (25) (a) Becke, A. D. *J. Chem. Phys.* **1993**, *98*, 5648. (b) Lee, C.; Yang, E.; Parr, R. G. *Phys. Rev. B* **1988**, *37*, 785. (c) Stevens, P. J.; Devlin, F. J.; Chablowski, C. F.; Frisch, M. J. *J. Phys. Chem.* **1994**, *98*, 11623.
- (26) (a) Krishnan, R.; Binkley, J. S.; Seeger, R.; Pople, J. A. *J. Chem. Phys.* **1980**, *72*, 650. (b) Frisch, M. J.; Pople, J. A.; Binkley, J. S. *J. Chem. Phys.* **1984**, *80*, 3265.

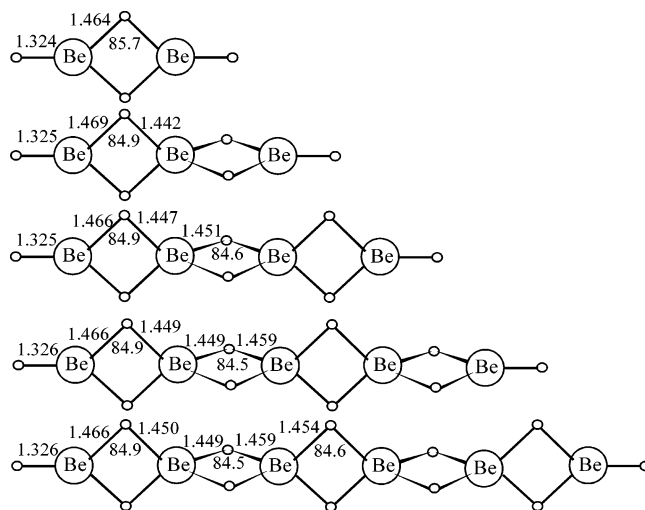
Table 2. Comparison of B3LYP-Calculated and Neon Matrix Observed Frequencies (cm^{-1}) for BeH_2 and $\text{HBe}(\mu\text{-H})_2\text{BeH}$

molecule, mode	calcd	obsd	scale factor
BeH_2 , antisym Be–H str, σ_u	2263	2172	0.960
HBeH bend, π_u	724	708	0.979
Be_2H_4 , terminal Be–H str, b_{1u}	2152	2065	0.960
bridge Be–H–Be str, b_{2u}	1598	1577	0.987
bridge Be–H–Be str, b_{1u}	1488	1423	0.956
Be–H–Be bend, out-of-plane, b_{3u}	952	923	0.970
Be–H–Be bend, in-plane, b_{2u}	589	585	0.993

Experiments were done with pure normal hydrogen ($n\text{-H}_2$) and deuterium ($n\text{-D}_2$). In solid hydrogen, strong BeH_2 bands appeared at 2165.3 and 706.3 cm^{-1} upon deposition and increased 5-fold upon broadband photolysis. A weak band at 1422.7 cm^{-1} observed upon deposition increased markedly upon photolysis while a group of bands formed just below this band (see Figure 1). Experiments with deuterium give spectra with similar behavior and H/D frequency ratios appropriate for light metal hydride vibrations. Weak BeH and BeD bands were observed at 1978.3 and 1481.4 cm^{-1} in normal H_2 and D_2 , respectively.

The infrared identification of Be_2H_4 [$\text{H}-\text{Be}(\mu\text{-H})_2\text{Be}-\text{H}$] is straightforward based on comparison with calculated frequencies and our early experiments in solid argon, which gave a strong diagnostic absorption at 1420 cm^{-1} .¹² The stronger 1422.9 cm^{-1} and weaker 1576.9 cm^{-1} bands in solid neon are located in the bridge stretching region, and antisymmetric $\text{Be}(\mu\text{-H})_2\text{Be}$ bridge-bond stretching modes parallel and perpendicular to the Be–Be axis, respectively, are proposed. The associated Be–H stretching and out-of-plane and in-plane Be–H–Be bending modes were observed at 2065, 922.9, and 584.6 cm^{-1} . In solid normal hydrogen, the bridge-bond stretching modes appeared at 1422.7 and 1574.8 cm^{-1} and the terminal Be–H stretching mode at 2056 cm^{-1} . Analogous spectra were observed using D_2 in neon and solid D_2 , and the H/D frequency ratios are 1.295 and 1.279 for the strong parallel and perpendicular bridge stretching modes, which evidence considerable anharmonicity.

DFT calculations were performed for BeH_2 and Be_2H_4 . First, the IR-active stretching mode of BeH_2 is predicted at 2263 cm^{-1} with the B3LYP functional, which must be scaled by 0.960 to fit the neon matrix value. This is typical for B3LYP frequency calculations.²⁷ Calculations at the same level performed for Be_2H_4 showed Be–H stretching at 2152 cm^{-1} and Be–H–Be stretching at 1488 and 1598 cm^{-1} , which match the neon experimental values with 0.960, 0.956, and 0.987 scale factors. Similar slightly different scale factors have been found for the two bridge stretching modes of $\text{H}_2\text{-Al}(\mu\text{-H})_2\text{AlH}_2$, namely, 0.949 and 0.981, respectively.¹⁷ Table 2 compares calculated and observed frequencies for $\text{HBe}(\mu\text{-H})_2\text{BeH}$. The strength of this identification is the match of five frequencies, and this agreement is as good as that observed recently for seven frequencies of $\text{H}_2\text{Al}(\mu\text{-H})_2\text{AlH}_2$.¹⁷ The appearance of lower-frequency satellite features on both bridge stretching modes following sample irradiation further relates these two absorptions.

**Figure 2.** Structures for $(\text{BeH}_2)_n$ polymers for $n = 2-6$ computed at the B3LYP/6-311++G(3df,3pd) level. Bond lengths are in angstroms, and bond angles are in degrees.

Polymeric $(\text{BeH}_2)_n$ species are formed in both solid neon and hydrogen. Ultraviolet irradiation markedly increased BeH_2 absorptions, and new bands just below the absorptions of Be_2H_4 in the Be–H–Be stretching region increased in concert, as shown in Figure 1. The yield of these new bands depends on the concentration of BeH_2 . Upon deposition of laser-ablated Be, weak BeH_2 absorptions and weak Be_2H_4 absorptions were observed. Clearly, not enough BeH_2 is generated upon deposition to form much polymer. However, the BeH_2 absorption increased upon ultraviolet irradiation using $\lambda > 350$, 240–380, and 220 nm (Figure 1), and additional satellite absorptions (1410–1330 cm^{-1}) also increased stepwise. Weak absorptions at 2056, 1556, 867, and 573 cm^{-1} also followed suit. Similar behavior was observed in neon matrix experiments, but the overall yield was less than that in pure hydrogen. In D_2 experiments, deuterium counterpart bands were found for the first four satellite absorptions as D_2 is less reactive than H_2 in these low-temperature experiments.

DFT calculations were done to model the structures of BeH_2 polymers. With B3LYP calculations, both single-bridged Be–H–Be (cyclic) and double-bridged Be– $(\mu\text{-H})_2$ –Be (linear) molecules converged, but double-bridged conformers were lower in energy. The central Be atom with four bonded H atoms in the optimized double-bridged Be_3H_6 molecule has a tetrahedral structure with all four equal Be–H bonds (1.442 Å), and the center bridge bonds increased to 1.451 Å for Be_4H_8 . Computed structures for $n = 2-6$ are illustrated in Figure 2. For Be_5H_{10} – Be_8H_{16} , the second and successive bridge bonds are computed in the 1.448–1.459 Å range. These structures alternate D_{2h} (even) and D_{2d} (odd) and show little change for $n = 5-8$. As the chain becomes longer, the bridged Be–H distance stands around 1.45 Å, which is comparable to theoretical values for the Be–H bond length in the polymer.⁸ We note that this is longer than the tetrahedral Be–H bond in the crystal (1.38 Å).⁵

The strongest IR-active modes for BeH_2 polymer are computed to be double-bridged Be–H–Be stretching modes,

(27) Bytheway, I.; Wong, M. W. *Chem. Phys. Lett.* **1998**, *282*, 219.

Table 3. Strongest Infrared Active Frequencies (cm⁻¹) Calculated for Linear (BeH₂)_n Polymers^a

molecule	frequencies, cm ⁻¹ (infrared intensities, km/mol) ^b
Be ₂ H ₄ , ¹ A _g <i>D</i> _{2h}	2152 (407), 1598 (255), 1488 (593), ^c 952 (243), 589 (157), 319 (229)
Be ₃ H ₆ , ¹ A ₁ <i>D</i> _{2d}	2152 (459), 1622 (193 × 2), 1522 (1429), 881 (92 × 2), 587 (97 × 2)
Be ₄ H ₈ , ¹ A _g <i>D</i> _{2h}	2151 (470), 1524 (1705), 1478 (1042), 890 (198), 587 (158)
Be ₅ H ₁₀ , ¹ A ₁ <i>D</i> _{2d}	2150 (482), 1609 (356 × 2), 1480 (3889), 887 (94 × 2), 588 (83 × 2), 497 (108 × 2)
Be ₆ H ₁₂ , ¹ A _g <i>D</i> _{2h}	2150 (488), 1609 (632), 1480 (1997), 1460 (3682), 888 (186), 588 (161), 499 (226)
Be ₇ H ₁₄ , ¹ A ₁ <i>D</i> _{2d}	2149 (492), 1608 (545 × 2), 1453 (7074), 888 (92 × 2), 589 (82 × 2), 510 (92 × 2)
Be ₈ H ₁₆ , ¹ A _g <i>D</i> _{2h}	2153 (495), 1608 (845), 1468 (340), 1442 (8545), 888 (181), 587 (159), 506 (211)

^a Calculation: B3LYP/6-311++G(3df,3dp). ^b Only the strongest terminal Be–H, perpendicular Be–H–Be, and parallel Be–H–Be stretching modes and Be–H–Be bending modes are listed. ^c Strongest parallel stretching mode absorptions are in bold.

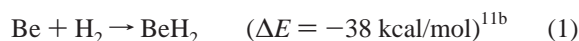
which are located in the same region as found for Be₂H₄. The observed polymer values decrease steadily from the dimer values (1577 and 1423 cm⁻¹ for Be–H–Be vibrations perpendicular and parallel to the chain axis), but fewer polymer bands are observed for the perpendicular than for the very strong parallel modes. Infrared spectra for the very strong parallel modes in the 1410–1330 cm⁻¹ region (Figure 1) are quite clear: Sequential ultraviolet irradiation increases the higher-frequency bands first and then the lower-frequency bands in the series with monotonically decreasing intensities. The B3LYP-calculated polymer frequencies (Table 3), which must be considered approximate, show slightly higher values for the trimer and tetramer before turning down as polymer length increases. The tetramer and hexamer have two very strong parallel bands that should, in principle, be observable, and many bands and shoulder absorptions are found in the polymer region, so it is possible that two bands might be due to Be₄H₈ and to Be₆H₁₂. However, for *n* = 7 and 8, one very strong absorption dominates the spectrum, and these bands decrease steadily in frequency with increasing *n* value. We cannot make a definitive assignment of a particular band to a particular higher polymer, but our spectra most likely contain (BeH₂)_n polymers up to at least *n* = 8. Hence, the calculated frequencies support the general assignment of these 1410–1330 cm⁻¹ infrared bands to (BeH₂)_n polymers in the solid matrix samples. We note that mixed alkyl beryllium hydride complexes exhibit Be(μ-H)₂Be bridge stretching modes in the 1340 cm⁻¹ region.²⁸

Our (BeH₂)_n calculations also predict terminal Be–H stretching and bending modes and bridge Be–H–Be bending modes immediately below the analogous modes computed for HBe(μ-H)₂BeH. Weak bands are observed at 2056, 867–864, and 572–558 cm⁻¹ for these modes of (BeH₂)_n polymers.

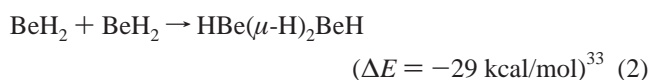
Upon evaporation of the hydrogen matrix containing BeH₂ molecules and (BeH₂)_n polymers, broad 1790, 1390, and 810 cm⁻¹ absorptions appear on the cold window, and a like treatment of the deuterium sample produces broad 1315,

1060, and 580 cm⁻¹ bands. These broad absorption bands are due to amorphous solid BeH₂ and BeD₂ materials, which begin to decompose at 170–180 K under vacuum. Similar infrared spectra have been observed for the amorphous solids at room temperature synthesized by dialkylberyllium pyrolysis.^{6,29}

The spectra in Figure 1 show that λ > 350 and 240–380 nm excitation of Be in solid H₂ increase the BeH₂ absorption bands. These wavelengths access the ³P states (455 nm in the gas phase).³⁰ Although this is a spin-forbidden transition, prolonged irradiation with an intense lamp does increase the BeH₂ yield. This energy is more than enough to surpass the computed 49 kcal/mol barrier¹⁴ for exothermic reaction 1. However, the ¹P state observed in absorption for Be in solid argon (236 nm) and neon (232 nm)³¹ is fully allowed, and full arc irradiation (λ > 220 nm) increases the BeH₂ bands even more efficiently. Once formed in the matrix by photochemical reaction, BeH₂ can be trapped as the isolated molecule or diffuse and associate to form (BeH₂)₂ dimer and (BeH₂)_n polymers. There is no evidence for H₂ ligand vibrations for a possible BeH₂ complex like those observed for (H₂)_nMgH₂.²¹ The lack of H₂ affinity for BeH₂ matches that for the beryllium metal surface.³²



After 240–380 nm irradiation, annealing to 6.8 K reduced the 2165 cm⁻¹ BeH₂ absorption by 23% and increased the 1423 cm⁻¹ Be₂H₄ band by 43%. Clearly, the exothermic dimerization reaction 2 proceeds without activation energy. However, the growth of higher polymer is limited upon annealing, but the major growth of (BeH₂)_n occurs upon λ > 220 nm irradiation, which produces new excited molecules to diffuse and react to form polymers. The average polymerization energy computed by DFT for polymers *n* = 2–8 is 33 kcal/mol, which is lower than the 39 kcal/mol value calculated at higher levels of theory for the one-dimensional system.⁸



In summary, we have prepared one-dimensional (BeH₂)_n polymers (Figure 2) by aggregation of the BeH₂ and HBe(μ-H)₂BeH molecules in solid neon and hydrogen. New infrared absorptions show that these polymers contain Be–H–Be bridge bonds of the type thought to be involved in the solid^{1–4}

(29) Yarger, J. L. University of Wyoming, Laramie, WY. Unpublished results, 2004.

(30) Moore, C. E. *Atomic Energy Levels*; National Bureau of Standards Circular 467; National Bureau of Standards, U.S. Government Printing Office: Washington, DC, 1952.

(31) Brom, J. W., Jr.; Hewett, W. D., Jr.; Weltner, W., Jr. *J. Chem. Phys.* **1975**, *62*, 3122.

(32) Ray, K. B.; Hannon, J. B.; Plummer, E. W. *Chem. Phys. Lett.* **1990**, *171*, 469.

(33) Other DFT calculations (Mire, L. W.; Wheeler, S. D.; Wagenseller, E.; Marynick, D. S. *Inorg. Chem.* **1998**, *37*, 3099) report slightly higher 31–35 kcal/mol values.

(28) Bell, N. A.; Coates, C. E. *J. Chem. Soc.* **1965**, *74*, 692.

until a definitive crystal structure measurement of a three-dimensional orthorhombic lattice with interconnected BeH_4 tetrahedra was made.⁵ When the matrix evaporates, these intermediate $(\text{BeH}_2)_n$ polymers react to form an amorphous BeH_2 solid with characteristic broad infrared absorptions.

Acknowledgment. We gratefully acknowledge support for this work from NSF Grant CHE 03-52487 and helpful correspondence with J. L. Yarger of unpublished results.

IC048464B